International Journal of Nanomedicine

Dovepress
open access to scientific and medical research

Open Access Full Text Article

ORIGINAL RESEARCH

A SARS-CoV-2 Nanobody Displayed on the Surface of Human Ferritin with High Neutralization Activity

Wenrong Zhang[1,2,*], Haining Wang[1,*], Tong Wu[1], Xintao Gao[1], Yuting Shang[1], Zhifang Zhang[1], Xingjian Liu[1], Yinü Li[1]

[1]National Key Laboratory of Agricultural Microbiology, Biotechnology Research Institute, Chinese Academy of Agricultural Sciences, Beijing, People's Republic of China; [2]College of Life Sciences, Capital Normal University, Beijing, People's Republic of China

*These authors contributed equally to this work

Correspondence: Xingjian Liu; Yinü Li, Tel/Fax +861082109854; +861082105495, Email liuxingjian@caas.cn; liyinv@caas.cn

Purpose: COVID-19 is rampant throughout the world, which has caused great damage to human lives and seriously hindered the development of the global economy. Aiming at the treatment of SARS-CoV-2, in this study, we proposed a novel fenobody strategy based on ferritin (Fe) self-assembly technology.

Methods: The neutralizing nanobody H11-D4 of SARS-CoV-2 fused to the C-terminus of end-modified human ferritin was expressed in *E. coli* and silkworm baculovirus expression systems. A large number of nanoparticles were successfully self-assembled in silkworms, while relatively few nanoparticles can be observed in the treated products from *E. coli* by electron microscopy. Subsequently, the fenobody's expression level and neutralizing activity were then evaluated.

Results: The results showed that the IC_{50} of H11-D4 and fenobody Fe-H11-D4 expressed in *E. coli* were 171.1 nmol L^{-1} and 20.87 nmol L^{-1}, respectively. However, the IC_{50} of Fe-HD11-D4 expressed in silkworms was 1.46 nmol L^{-1} showing better neutralization activity.

Conclusion: Therefore, fenobodies can be well self-assembled in silkworm baculovirus expression system, and ferritin self-assembly technology can effectively improve nanobody neutralization activity.

Keywords: COVID-19, ferritin, fenobody, baculovirus expression system, silkworm

Introduction

Since 2020, novel coronavirus disease (COVID-19) caused by SARS-CoV-2 has broken out in the world. It is very important to develop a new and effective antibody to cope with the COVID-19 pandemic. SARS-CoV-2 viruses are particles approximately 80–120 nanometres in diameter, and the presence of spikes on the surface is a distinguishing feature of this virus as a member of the Coronaviridae family.[1] The receptor-binding domain RBD of S protein on the surface of the SARS-CoV-2 virus binds to the receptor ACE2 on the body's cell membrane, allowing the virus to enter the body.[2]

At present, the control strategy of SARS-CoV-2 mainly depends on the vaccine and antibody against spike (S) protein. Various vaccines have been put on the market, including inactivated vaccines, vector vaccines, recombinant sub-vaccine, etc. The antibody is another very important research strategy and has a broad research prospect. The research of antibodies has evolved from conventional antibodies to single-chain antibodies to nanobodies, and nanobodies are becoming an emerging hot field in antibody development with widespread and sustained attention due to their unique physical and chemical stability and greater suitability for large-scale production.[3] Nanobodies were first proposed in 1993 with the discovery of the variable domain of heavy chain (VHH) alone expression of a heavy chain antibody from camelid bodies[4] had a stable structure and strong antigen binding ability.[5]

Accumulating works indicate that the modified nanobodies have the advantages of weaker immunogenicity, stronger penetration,[6] better stability, and higher affinity, and their preparation method is simpler, which has great development

Received: 4 December 2023
Accepted: 29 February 2024
Published: 8 March 2024

potential.[7] Recently, several strategies have been used to develop nanobodies, the nanobody Ty1[8] can be expressed in large quantities in bacteria and specifically targets RBD protein, and its binding to RBD directly blocks the binding between RBD and ACE2. The RBD-binding nanobody H11 was identified in the original alpaca VHH library, and the nanobody H11-D4 was proved to bind to RBD with a KD (dissociation constant) of 39±2 nmol L^{-1}, and then it was fused with the Fc segment of IgG protein to carry out the pseudovirus neutralization experiment at the cell level. The results showed that the IC_{50} of H11-D4-Fc was 161 nmol L^{-1}. This undoubtedly provides an effective anti-COVID-19 method and an excellent candidate drug for the treatment and prevention of COVID-19.[9]

Ferritin can be used as the backbone of nanoparticles because of its advantages in protein display and antigen presentation, and it is a new strategy for preparing high-efficiency antibodies. For instance, the anti-H5N1 nanobody was displayed on the surface of ferritin from archaea in the form of 24-mer,[10] and researchers found that its affinity with antigen increased by more than 300-fold, and its half-life in mice was about 10-fold longer than that of the anti-H5N1 nanobody alone, and then they named this chimera protein fenobody. In 2021, two subunit vaccine candidates were designed based on self-assembled ferritin nanoparticles to display the full-length outer domain (S-Fer) or 70 amino acid deletion (SΔC-Fer) of poly-SARS-CoV-2 spikes,[11] and researchers found that fusion expression with ferritin improved the protein expression level.

Ferritin nanoparticles can self-assemble into stable structures[12] with remarkable thermal and chemical stability and can be used as drug delivery carriers and scaffolds to display exogenous peptides or proteins.[13] It is important for the development of new drugs. Ferritin is conserved, and human ferritin is one of the classical ferritins with a protein shell that is self-assembled from heavy chains (H-chain, 21 kDa) and light chains (L-chain, 19 kDa).[14] However, individual heavy chains can also self-assemble into ferritin with high efficiency.[15] In this study, the human ferritin heavy chain was chosen as the antibody carrier, which is expected to be more suitable for human use and has lower immunogenicity.

The baculovirus expression system has become a mature production platform for producing viral vaccines and gene therapy vectors.[16] Compared with mRNA and adenovirus vector vaccines, COVID-19 vaccines developed by the baculovirus expression system[17] have certain advantages in safety, production cost, and vaccine storage temperature. The target protein from insect cells has a correct protein folding and can be modified by post-translation processing, glycosylation, and phosphorylation.[18] Therefore, the silkworm baculovirus expression system was used to produce fenobodies efficiently and cheaply in silkworms, and the activity of fenobodies was evaluated.

Materials and Methods

E. coli competent cells DH5α and Rosetta (DE3) were purchased from TransGen Biotech, Beijing, China. Prokaryotic expression vector pET28a were preserved in our laboratory. The human embryonic kidney cells (HEK-293T) were obtained from ATCC. The pcDNA3.1-hACE2-GFP plasmid, pcDNA3.1-S plasmid and pNL4-3.Luc.R-E plasmid are preserved in our laboratory. The gene sequence needed in the experiment was codon optimized and synthesized by GenScript, Nanjing, China.

Construction of Recombinant Expression Vector

Prokaryotic Expression Vectors pET28a-H11-D4 and pET28a-Fe-H11-D4 for Nanobody and Fenobody

The amino acid sequence of SARS-CoV-2 neutralizing nanobody H11-D4 (PDB: 6YZ5_F) and the amino acid sequence of human ferritin heavy chain (GenBank: AAA35832.1) were selected from the database. To promote the better fusion of nanobody H11-D4 with human ferritin, the following design method was determined by the prediction of Alphafold:[19] the N-terminal 5 and C-terminal 21 amino acids of ferritin, the C-terminal 6 amino acids of H11-D4 were removed. The H11-D4 protein sequence was fused to the C-terminal of ferritin by a linker (GGGSGGGGSGGGS). After codon preference optimization, restriction enzyme sites *Bam*H I and *Eco*R I were added to both ends of the optimized nucleotide sequence. Subsequently, H11-D4 and Fe-H11-D4 fragments (Phanta Max ultra-fidelity DNA polymerase was purchased from Vazyme) were amplified by fusion PCR. The fragments were then connected to the pET28a vector through *Bam*H I and *Eco*R I to construct pET28a-H11-D4 and pET28a-Fe-H11-D4.

Construction of Recombinant Silkworm Baculovirus with Nanobody and Fenobody

The H11-D4 and Fe-H11-D4 fragments were amplified via enzyme digestion and cloned into the pBR vector[20] to obtain transfer vectors pBR-H11-D4 and pBR-Fe-H11-D4. Inactivated rescue baculovirus DNA was co-transfected into cells with baculovirus transfer vectors pBR-H11-D4, pBR-Fe-H11-D4, and pBR-Luc control, respectively[21] (VigoFect was purchased from Vitality Biotech Beijing Co., Ltd. in Beijing, China). Finally, the recombinant BmNPV baculoviruses reBm-H11-D4 and reBm-Fe-H11-D4 were obtained from the supernatants of the cotransfected cells, based on which the recombinant viruses were screened, purified, amplified, and retained as viral stocks.

Expression and Purification of H11-D4 and Fe-H11-D4

In terms of *E. coli* expression, the recombinant plasmids pET28a-H11-D4 and pET28a-Fe-H11-D4 were transformed into *E. coli* expression strain Rosetta (DE3). Monoclone was picked and cultured in liquid LB medium with the kana antibiotic at 37 °C for about 12 h. According to the ratio of 1%, monoclone was transferred into a new liquid medium for further cultivation. After optimization, the bacterial broth was cultured until the OD_{600} was between 0.6 and 0.8, and the expression products were obtained by adding 1.0 mmol/L IPTG and analyzed using SDS-PAGE. The fusion protein was then expressed and purified via Ni-NTA affinity purification. To assemble the Fe-H11-D4 protein spherical nanostructures, the fusion protein was refolded in dialysis buffer (Fe^{3+} with an appropriate concentration) with a gradually decreased urea concentration. Then, 1% Triton X-11 was added to the supernatant of the renatured proteins to remove endotoxin, concentrated by ultrafiltration using an ultrafiltration tube, quantified, and diluted to 1 mg/mL.

In terms of silkworm expression, the recombinant virus (10^5 PFU) was injected into the dorsoventral internode of 5th instar silkworm larvae or pupae and then continued rearing or incubation at 25–27 °C and 65% humidity. After 96 h of rearing and observation of typical baculoviral symptoms in the silkworm, silkworm hemolymph was collected by puncturing the ventral foot of the silkworm and frozen preservation. The supernatant of the sample of silkworms expressing fenobody after ultrasonic crushing and high-speed centrifugation to remove cell debris. The crude samples were purified by gentle ultrasonic crushing and ultracentrifugation using a 30% sucrose cushion at 120,000 g for 3 h. The white transparent nanoparticle pellets were resuspended in PBS overnight.

Identification and Quantitative Determination of H11-D4 and Fe-H11-D4

Identification of the products of prokaryotic expression, the purified H11-D4 and Fe-H11-D4 proteins were validated by Western blot using mouse-derived His-tag primary antibody (TransGen Biotech, Beijing, China) and HPR-labeled goat anti-mouse IgG secondary antibody (ZSGB-BIO, Beijing, China). To verify the purified targeted proteins, the purified proteins were subjected to SDS-PAGE. The properly sized protein bands were excised and forwarded to the central laboratory of the Biotechnology Research Institute of the Chinese Academy of Agricultural Sciences (CAAS) for LC-MS -MS analysis, specifically utilizing the Orbitrap Fusion instrument.

H11-D4 and Fe-H11-D4 proteins expressed in *E. coli* were purified using the Ni-NTA affinity purification method and quantified using the BCA protein assay kit.

Identification of the products of eukaryotic expression, the products expressed in silkworms were ultrasonically disrupted, and cell debris was removed by centrifugation. The supernatant was then used to determine the amount of recombinant protein expressed in silkworms by ELISA. The prokaryotic expression of Fe-H11-D4 protein was embedded in the enzyme label plate at the concentrations of 5 μg/mL, 1 μg/mL, 0.5 μg/mL, and 0.1 μg/mL; then, Fe-H11-D4 expressed in silkworm and the corresponding treated negative samples of Bm-Luc were coated with gradients at serial dilutions, respectively. After overnight incubation at 4 °C, plates were washed thrice with PBST, a blocking buffer containing 1% BSA in PBST was added, and the plates were incubated for 1 h at room temperature. After 1 h of incubation at 37 °C, the plates were washed thrice, and HRP-conjugated goat anti-mouse IgG antibody was added at a dilution ratio of 1:5000. After incubation for 1 h at 37 °C, the plates were washed thrice with PBST and developed with TMB (Sigma-Aldrich (Shanghai) Trading Co. Ltd.) for 10 min. The reaction was stopped using a stop solution (1 M H_2SO_4). The absorbance was measured at 450 nm using a microplate reader.

The concentration of recombinant proteins expressed by silkworms was determined by using human ferritin heavy chain rabbit primary antibody (purchased from ABclonal Biotechnology Co., Ltd.) and HRP-labeled goat anti-rabbit IgG secondary antibody.

Electron Microscope Observation

A transmission electron microscopy (Tecnai G2 F20 TWIN TMP) was used to observe whether the nanoparticles self-assembled successfully. Negative staining and transmission electron microscopy were performed on the purified protein expressed in *E. coli* and the crude purified protein expressed in silkworms, respectively. Immunogold labeling was used to determine whether H11-D4 proteins were present on the surfaces of the nanoparticles, which were incubated with a 50-fold dilution of ferritin monoclonal antibody for 10 min and with a 50-fold dilution of goat anti-rabbit IgG gold-10nm antibody (purchased from SIGMA-ALDRICH) for 10 min and stained with uranium acetate under the electron microscope.

Construction of SARS-CoV-2 Pseudovirus and Neutralization Test

Following the methodology of reference,[22] to construct SARS-CoV-2 pseudovirus (original Wuhan-Hu-1 strain, RefSeq: YP_009724390.1), pcDNA3.1-S plasmid and pNL4-3.Luc. R-E plasmid were transfected into 293T cells, and the viral supernatant was collected. To assess the neutralization of pseudovirus infection in vitro, 293T cells were seeded in 96-well plates and grown overnight, and the pcDNA3.1-hACE2-GFP plasmid was transfected into 293T cells according to the VigoFect instructions. The plasmid transfection was confirmed by observing fluorescence 24h after transfection. The H11-D4, Fe-H11-D4, and BSA samples were preincubated with an equal volume of pseudoviruses of SARS-CoV-2 origin, respectively. DMEM was mixed with an equal amount of pseudovirus as a positive control, DMEM-only wells were used as a negative control, and three replicate wells per sample. After incubation, the mixture was added to hACE2-expressing cells, and then the cells were suspended with lysis buffer (Promega), after collection, the nanobody was mixed with luciferin, and the expression of firefly luciferase (relative light unit, RLU) was detected by luminometer (Promega, GloMax® 20/20). The inhibition rate of pseudovirus entry into cells was calculated.[23] Inhibition rate = (experimental group RLU-negative control group RLU)/(positive control group RLU-negative control group RLU)×100%.

Results

Expression of H11-D4 and Fe-H11-D4

Ferritin can generally be modified at the C-terminal or N-terminal and is originally an 8-trimer nanoparticle, while the trimer structure does not conform to the natural nanobody conformation. To obtain better display results, we designed various forms of fusion methods. The three-dimensional structural prediction analysis of nanobody was performed via the AlphaFold program and PyMol software. It was speculated that the heavy chain subunit of human ferritin (N-terminal removal of the first 5 amino acids and the C-terminal removal of 21 amino acids of ferritin) would convert the displayed triple-petal-like structure into a homodimeric structure, and to promote a better fusion and expression of nanobody H11-D4 with human ferritin, the C-terminal 6 amino acids of H11-D4 were removed, and the GGGSGGGGSGGGS was used as a linker added to the N-terminal of H11-D4, thereby obtaining the possible dimer nanobodies displayed on the surface of human ferritin nanoparticles, and each nanoparticle can display six (2X2) nanobody clusters on the surface of human fenobody (Figure 1), which basically conforms to the spatial structural form required for highly active fenobodies.

After codon preference optimization, the plasmids pUC57-linker-H11-D4 and human Ferritin plasmid pUC57-Fe were obtained by synthesis, and the H1-D4 gene was obtained by PCR using pUC57-linker-H11-D4 as a template, and cloned into the prokaryotic expression vector pET28a by digestion of *Bam*H I and *Eco*R I to obtain pET28a-H1-D4; The Fe-H11-D4 gene was obtained by fusion PCR using pUC57-linker-H11-D4 and pUC57-Fe as templates, and cloned into the prokaryotic expression vector pET28a by digestion of *Bam*H I and *Eco*R I to obtain pET28a-Fe-H1-D4. Then, the above expression plasmid was transformed to Rosetta (DE3) strains for expression and obtained H11-D4, Fe-H11-D4 protein.

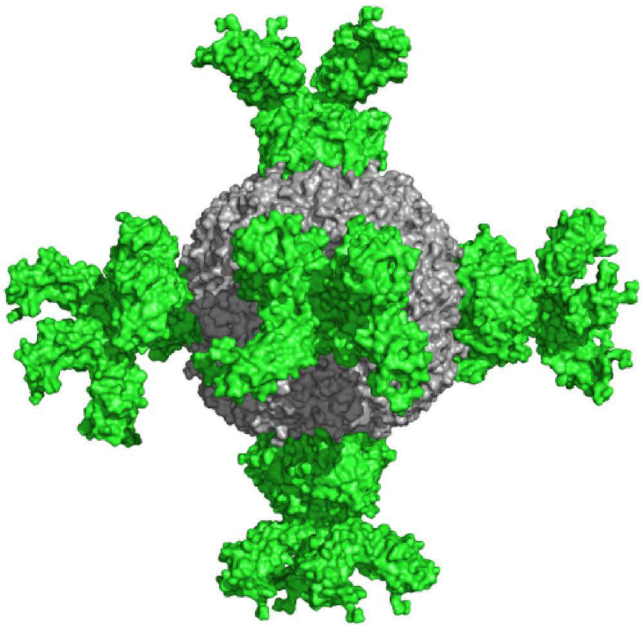

Figure 1 Structural prediction of nanobody H11-D4 fused with the heavy chain of human ferritin fusion protein.

The H11-D4 and Fe-H11-D4 genes were cloned into the baculovirus transfer vector pBR and identified the pBR-H11-D4 and pBR-Fe-H11-D4 plasmids by digestion and sequencing, which demonstrated the successful construction of transfer plasmids driven by the promoter of the polyhedrin gene, and co-transfected in Bm-N cells of silkworms with inactivated rescuing baculoviral DNA, and cultured the cells for 5 d. After 5 d of incubation, compared with normal cells (Figure 2a), the co-transfected cells showed typical pathological effects caused by baculovirus, such as aggregation and suspension (Figure 2b). Similarly, pBR-Luc DNA was used for co-transfection as a quality control standard for the process of viral recombination, and the supernatant was collected to detect the luciferase expression of the reBmBac-Luc group which reached more than 8 million CPM (15 microlitres), which proved that the effect of co-transfection was good, and recombinant baculoviruses reBamBacFe-H11-D4 and reBamBacH11-D4 were obtained. The recombinant viruses were purified and amplified as virus stocks, and the silkworms were infected with them to collect the silkworm expression products. Accordingly, the recombinant viruses containing luc were also used as the quality control standard for the expression process in the silkworms, and the luciferase expression of the reBmBac-Luc group was detected to reach more than 60 million CPM, which indicated that the silkworms were healthy, free of contamination by the wild viruses, and suitable for expression of the target proteins.

Genomic DNA was extracted from silkworm expression samples infected with reBmBac-H11-D4, reBmBac-Fe-H11-D4, and reBmBac-Luc group, and verified the H11-D4 and Fe-H11-D4 genes by PCR. A clear single band appeared around 400bp and 900bp, respectively (Figure 2c), which was consistent with the size of the fragments of H11-D4 and Fe-H11-D4 genes, indicating that the target genes had been successfully integrated into the baculovirus genomes.

Western Blot Analysis and Mass Spectrometry Identification of the Expression Products H11-D4 and Fe-H11-D4

The prokaryotic expression products were detected by SDS-PAGE as shown in (Figure 3A and B). The results showed clear bands around both 17.9 kDa and 37.1 kDa, which were consistent with the predicted molecular weight size of the theoretical fusion proteins, and with a less soluble state and a large amount in the form of inclusion bodies. Subsequently, the fusion protein was expressed in large quantities, and the H11-D4 and Fe-H11-D4 proteins expressed in *E. coli* were purified by Ni-NTA affinity purification and carried out Western blot to verify the recombinant proteins, with His-tag primary antibody of murine origin, and HPR-labelled goat anti-mouse IgG secondary antibody, and the results of the

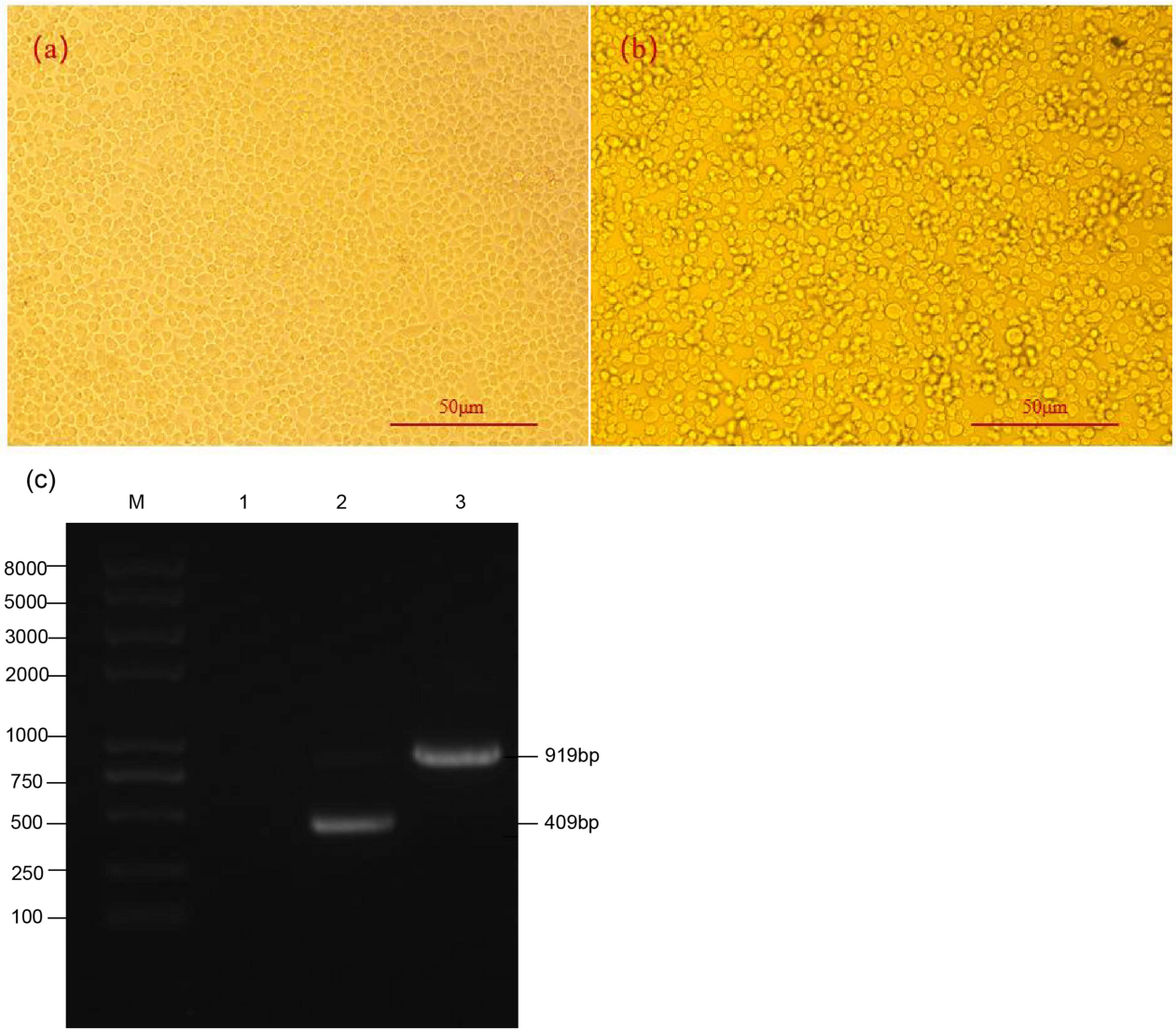

Figure 2 Construction of recombinant virus. (**a**) Normal cells; (**b**) Co-transfected cells; (c) M: DNA Marker; 1: PCR with reBmBac-Luc genome as template; 2: PCR with reBmBac-H11-D4 genome as template; 3: PCR with reBmBac-Fe-H11-D4 genome as template.

validation were as shown in Figure 3C. As shown in Figure 3C, there was a single obvious band around 18 kDa and 37 kDa in lanes 1 and 2, respectively. The molecular weights were consistent with the theoretical values, which proved that the recombinant proteins H11-D4 and Fe-H11-D4 were successfully expressed in *E. coli* after the purification of recombinant proteins by SDS-PAGE. The protein bands with correct sizes were cut, and sent to the central laboratory of CAAS, for LC-MS-MS analysis. The protein coverage for recombinant proteins H11-D4 and Fe-H11-D4, as revealed by the MS-MS analysis, is exceptionally high at 89.06% (Table S1) and 76.85% (Table S2), respectively. Additionally, 12 specific peptide sequences were identified for H11-D4, and 20 specific peptide sequences were identified for Fe-H11-D4 through successful amino acid sequence determination. The observed protein molecular weights and amino acid counts align with the theoretical values, confirming that the purified recombinant proteins are indeed H11-D4 and Fe-H11-D4.

The Fe-H11-D4 and H11-D4 proteins expressed in silkworms were subjected to ultrasonic fragmentation, centrifugation, and filtration after appropriate dilution, followed by Western blot verification. The results showed that the molecular weight of Fe-H11-D4 protein was 33.4 kDa. The results were consistent with the predicted molecular weight, indicating that Fe-H11-D4 protein was successfully expressed in the expression system of the silkworm (Figure 3D).

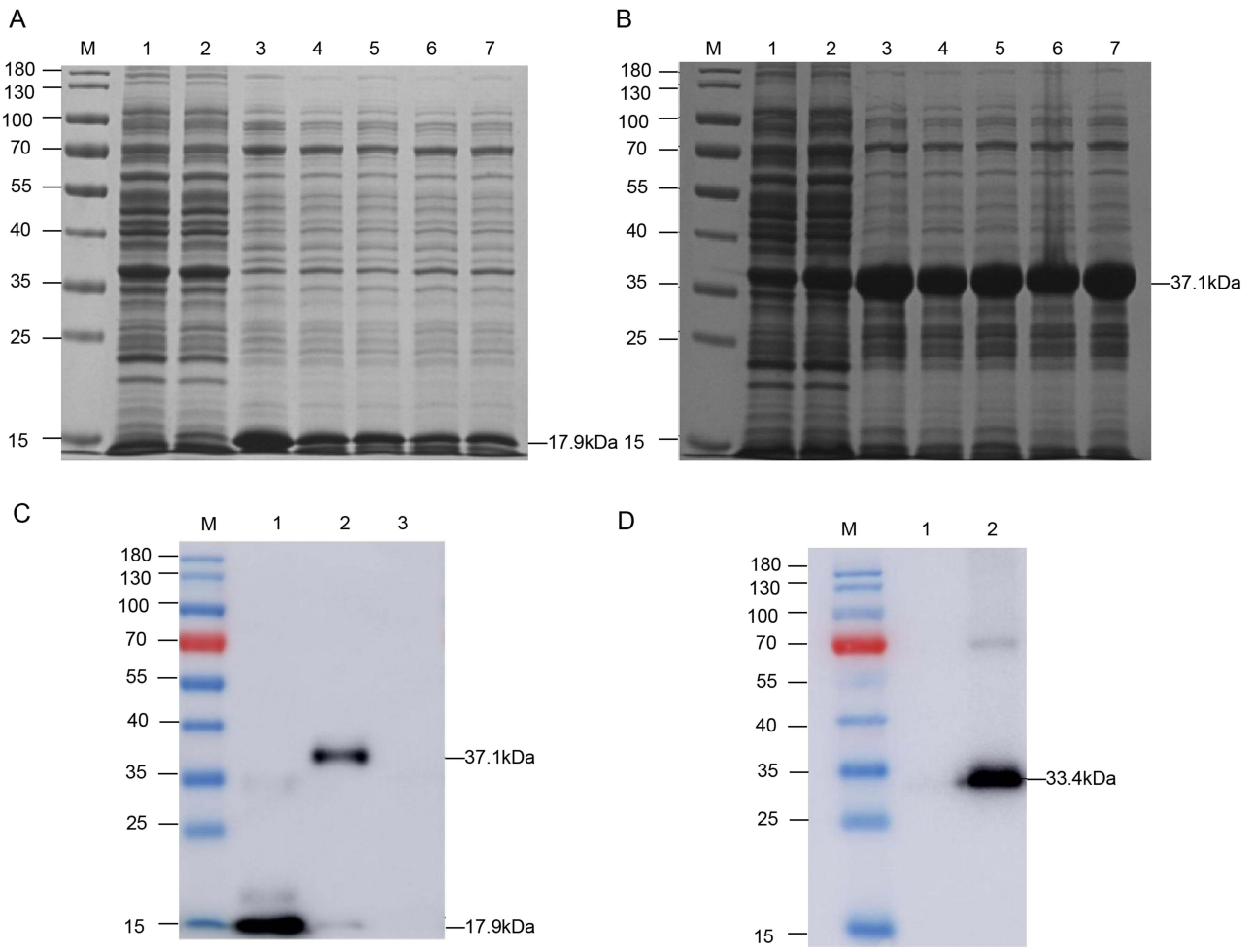

Figure 3 Expression of the H11-D4 and Fe-H11-D4 proteins. (**A**) SDS-PAGE analysis of recombinant pET-28a-H11-D4 in *E. coli*. M: protein marker 1: pET28a; 2: pET28a-H11-D4 (uninduced); 3: pET28a-H11-D4 (induced with 1.0 mmol/L); 4: pET28a-H11-D4 (induced with 0.8 mmol/L); 5: pET28a-H11-D4 (induced with 0.5 mmol/L); 6: pET28a-H11-D4 (induced with 0.3 mmol/L); 7: pET28a-H11-D4 (induced with 0.1 mmol/L); (**B**) SDS-PAGE analysis of recombinant pET-28a-Fe-H11-D4 in *E. coli*. M: protein marker; 1: pET28a; 2: pET28a-Fe-H11-D4 (uninduced); 3: pET28a-Fe-H11-D4 (induced with 1.0 mmol/L); 4: pET28a-Fe-H11-D4 (induced with 0.8 mmol/L); 5: pET28a-Fe-H11-D4 (induced with 0.5 mmol/L); 6: pET28a-Fe-H11-D4 (induced with 0.3 mmol/L); 7: pET28a-Fe-H11-D4 (induced with 0.1 mmol/L); (**C**) Western blot analysis of H11-D4 and Fe-H11-D4 recombinant proteins expressed in *E. coli*. M: protein marker; 1: pET28a-H11-D4; 2: pET28a-Fe-H11-D4; 3: pET28a unloaded; (**D**) Western blot analysis of Fe-H11-D4 recombinant proteins expressed in silkworm. M: protein marker; 1: infected reBmBac-Luc; 2: infected reBmBac-Fe-H11-D4.

Determination of Recombinant Protein Expression Levels of Fe-H11-D4 and H11-D4

The concentration of the purified protein was determined using a BCA protein quantification kit, and the standard curve $y = 0.001x+0.0413$ ($R^2 = 0.9959$) was plotted with the concentration of standard BSA as the x-axis and the absorbance value of OD_{562} as the y-axis, which showed a good linear relationship. The yields of recombinant proteins H11-D4 and Fe-H11-D4 per liter of the bacterial solution in the shake flask after purification were calculated as 25.16 μg/mL and 8.70 μg/mL based on the absorbance substitution into the formula. To determine the content of recombinant proteins expressed in the silkworm, we examined the expression level of the fusion protein Fe-H11-D4 by ELISA of the expression sample. The purified and quantified Fe-H11-D4 protein expressed in *E. coli* was used as the standard material, and human ferritin antibody as the primary antibody. The results showed that the expression level of Fe-H11-D4 was 101.23 μg/mL silkworm haemolymph detected by ELISA.

Electron Microscopic Observation of Fe-H11-D4

The inclusion bodies in the Fe-H11-D4 proteins expressed in *E. coli* were purified and refolded via dialysis and observed using the electron microscope. The results showed that the ferritin fusion H11-D4 was able to self-assemble into

a spherical structure of about 20 nm (Figure 4A), and further immunogold particle labeling of the ferritin showed that ferritin was located at the center of the spherical nanostructure. However, there are few nanoparticles in a field of vision. Even if some conditions are optimized during dialysis, such as adding a small amount of iron ions during the dialysate, there is no obvious effect, which shows that the method we adopted needs to be further improved, and the self-assembly efficiency of fenobodies is low in prokaryotic expression systems. The Fe-H11-D4 expressed by silkworm was observed by electron microscope after crude purification. It was observed that the fenobody Fe-H11-D4 was self-assembled into a natural spherical structure of about 20nm in silkworms (Figure 4B). The ferritin was located at the center of the spherical nanostructure and H11-D4 was displayed on the surface of ferritin, and there were more Fe-H11-D4 expressed by silkworms in a field of vision. These results show that the eukaryotic expression system of silkworms is more suitable for self-assembly ferritin technology than the prokaryotic expression system of *E. coli*.

Pseudovirus Neutralization Test Analysis

The inhibitory rates of H11-D4 and Fe-H11-D4 expressed in *E. coli* against viruses entering cells were calculated according to the detected luminescence counts, and the neutralization activity curves of H11-D4 and Fe-H11-D4 against pseudoviruses were drawn by using GraphPad Prism 8, as shown in Figure 5. The results showed that H11-D4 and Fe-H11-D4 could effectively inhibit pseudovirus from entering cells, and the inhibition rate increased with the increase of recombinant protein concentration, while the inhibition rate of BSA negative control was close to zero, and there was no ability to inhibit pseudovirus from entering cells. We calculated the 50% inhibitory concentrations (IC_{50}) of H11-D4 and Fe-H11-D4 by using GraphPad Prism 8, which were 171.1 nmol L^{-1} (Figure 5A) and 20.78 nmol L^{-1} (Figure 5B), respectively. The neutralizing activity of the fenobody is obviously higher than that of the nanobody expressed alone, which proves that the nanobody on the surface of ferritin improves the targeting affinity for the RBD domain of the S protein.

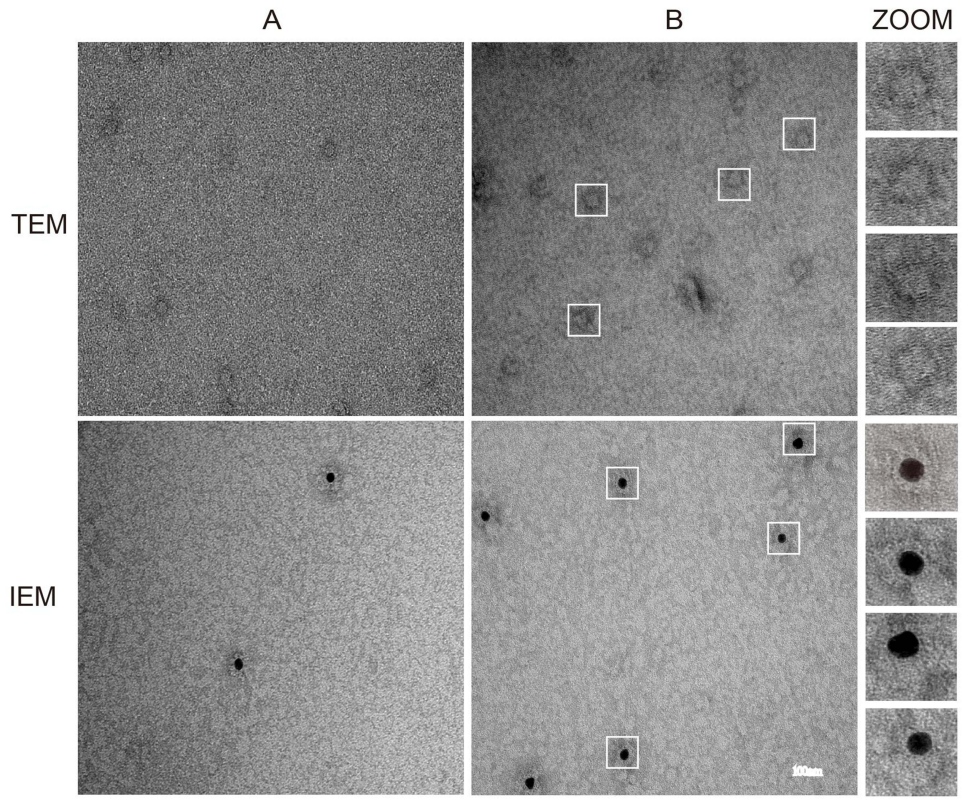

Figure 4 TEM and IEM analyzes of Fe-H11-D4 and electron microscopic observation of the nanoparticles. (**A**) Electron microscopic observation of *E. coli* expressing Fe-H11-D4. (**B**) Electron microscopic observation of Fe-H11-D4 expressed by silkworm (suitable diluted). Scale bar is 100 nm.
Abbreviations: TEM, transmission electron microscopy; IEM, immunoelectron microscopy.

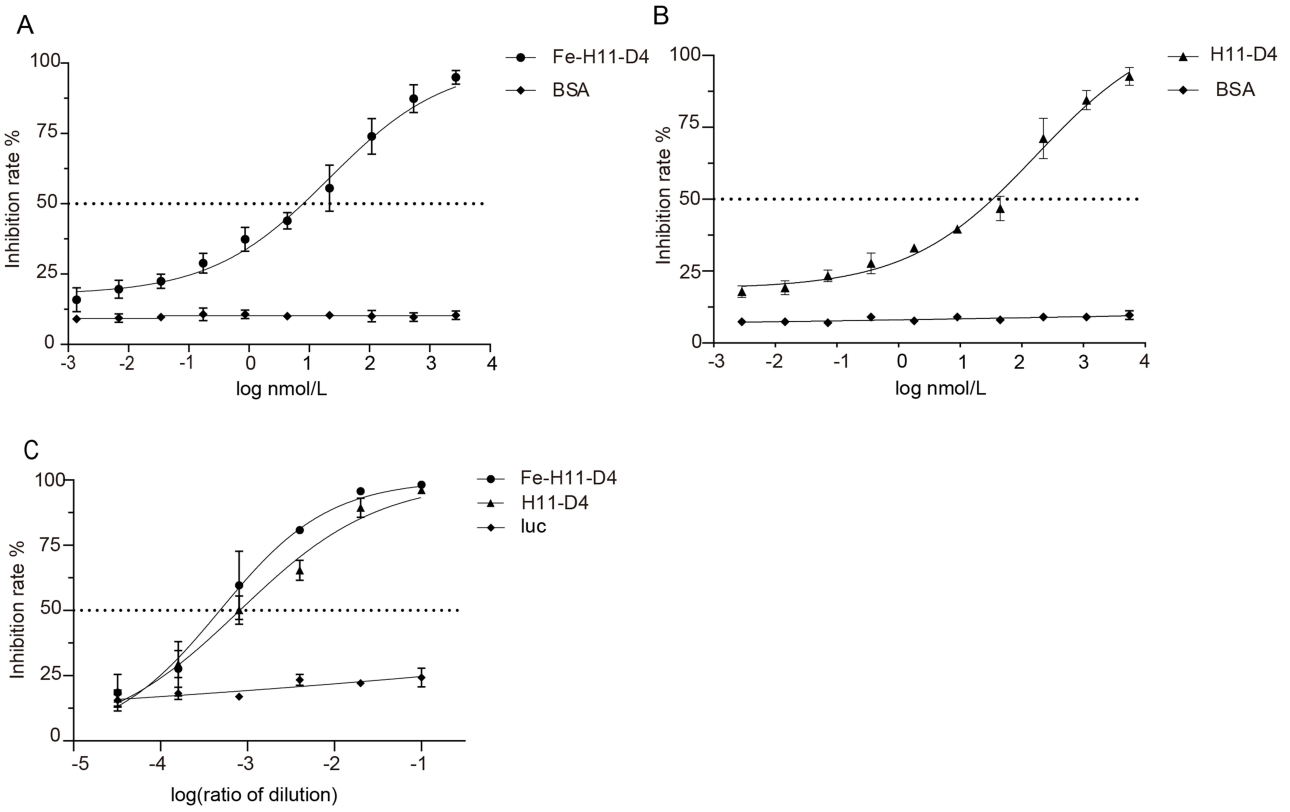

Figure 5 Pseudovirus neutralization test. (**A**) The half inhibitory concentration of H11-D4 expressed by *E. coli* was 171.1 nmol-L^{-1}; (**B**) The half inhibitory concentration of Fe-H11-D4 expressed by *E. coli* was 20.78 nmol-L^{-1}; (**C**) The half inhibitory concentration of Fe-H11-D4 expressed by Bombyx mori was 1.46 nmol-L^{-1}.

The neutralization titers of H11-D4 and Fe-H11-D4 in silkworm expression production were dilution ratios of 1:1226 and 1:2080. According to the concentration of Fe-H11-D4 protein in silkworm expression production, the IC_{50} of Fe-H11-D4 was calculated to be 1.46 nmol L^{-1} (Figure 5C), and the IC_{50} was significantly higher than that of Fe-H11-D4 expressed in prokaryotic expression production, which proved that the neutralization activity of fenobody expressed in silkworm samples was higher than that of fenobody purified and renaturated in prokaryotic expression production, reflecting the advantages of silkworm baculovirus in better self-assembly efficiency and post-translation processing.

Discussion

In the prophylaxis and treatment of COVID-19, conventional monoclonal antibodies generally suffer from long preparation periods and high preparation costs. In addition, the relatively large size of the antibodies also leads to low permeability, which affects their therapeutic effect, while nanobodies have a smaller molecular weight, better tissue penetration and weaker immunogenicity, and have a good stability. Therefore, nanobodies can be administered by inhalation, oral administration, infusion, and injection, which is especially suitable for the treatment of respiratory diseases,[24] and has promising potential as therapeutic[25,26] and diagnostic tools.[27] Moreover, nanobodies perfectly compensate for the deficiency of monoclonal antibody preparation and application due to their low production cost, easy modification and amplification,[3] and have great clinical application potential.

The three-dimensional structure of ferritin is highly conserved from bacteria to mammals,[15] prokaryotic ferritin has the feature that 24 monomers are assembled into nanoparticles, and eukaryotic ferritin reassembly also has this feature. Existing research suggests that bacterial ferritin was used to present preS1,[28] a protein structural domain on the surface of hepatitis B virus. PreS1 on the surface of bacterial ferritin can elicit a strong immune response and has good biosafety upon entry into the organism. Compared with other carriers, ferritin shows unique advantages, such as high heat resistance and water solubility, good biocompatibility, and other advantages, which make it has great prospect for

application in the fields of medicine, food, and so on.[29] In this study, human ferritin was similarly modified by changing the display mode of archaea ferritin (*P. furiosus* ferritin-nanobody by replacing the sequence encoding the helix ε and loop of the ferritin subunit with the nanobody sequence through a linker) as a nanobody carrier, which can reduce the immunogenicity in the human body. The heavy chain of human ferritin was predicted by Alphafold in the hope of modifying the displayed trimer-like structure to be able to display nanobodies on the surface.

After purification of the prokaryotic expression products, the successful expression of H11-D4 and Fe-H11-D4 in *E. coli* was confirmed by Western blot and Mass Spectrometry. Transmission electron microscopy showed that Fe-H11-D4 had a spherical structure with a diameter of about 20nm, and immunogold labeling showed that the gold particles were attached to the core of the spherical structure. Ferritin nanoparticles fused with nanobody H11-D4 could successfully self-assemble into spherical nanostructures in complexation. The better neutralization activity was further verified by the pseudovirus neutralization assay, and the IC_{50} of Fe-H11-D4 was 20.78 nmol-L^{-1}, which was 8-fold higher than that of the H11-D4 (IC_{50} 171.1 nmol-L^{-1}) expressed alone. The fenobody (a nanobody against H5N1 virus is displayed on the surface of ferritin in the form of a 24mer) TEM analysis showed that nanobodies were displayed on the surface of ferritin in the form of 6 × 4 bundles, and the clustered nanobodies are flexible in their spatial structure for antigen binding, the apparent antigen binding affinity of the anti-H5N1 fenobody was dramatically increased.[10] In this study, it is possible that ferritin can be accurately folded and displayed as a dimer by transforming the structure of human ferritin-heavy chain. Nanobodies are displayed on the surface of human ferritin nanoparticles, improving the structure and properties of the nanoparticles.

The prokaryotic-expressed fusion proteins were refolded via dialysis, and fewer particles were observed by electron microscopy. Even though various methods such as adding a small amount of ferric ions, temperature and protein concentration, etc. during the renature process were changed, but none of them had any significant effect, and the refolding efficiency of ferritin was low, which indicated that the method we used still needs to be further improved.

Analyzed from the perspective of different expression systems, the silkworm-expressed samples were crudely purified and then verified by Western blot and Electron Microscopy, and more nanoparticles could be observed in the field of view. The existing research shows that the ability of H11-D4-Fc to block the binding of RBD in MDCK cells stably expressing ACE, and the half-inhibitory concentration of H11-D4-Fc[9] was 161 nmol-L^{-1}. The IC_{50} of Fe-H11-D4 expressed in silkworms was calculated to be 1.46 nmol-L^{-1} compared to the prokaryotically expressed Fe-H11-D4 fusion protein (IC_{50} 20.78 nmol-L^{-1}), which has an almost 20-fold higher neutralizing activity. Results showed that there are two possible reasons for the better neutralization activity of fenobody expressed by eukaryotic systems, one is that the eukaryotic expression system has a post-translational modification function and is more conducive to the nanoparticle self-assembly than the prokaryotic expression system,[30] and another may be that nanobody is displayed on the surface of ferritin, which effectively improves the targeting affinity of nanobodies to RBD and the neutralizing activity of fenobody against pseudovirus.

The silkworm expressed H11-D4 was purified by various treatments, including high temperature and hydrochloric acid denaturation. Although it had little effect on the activity, its purity was not enough to quantify the silkworm-expressed H11-D4. The IC50 of H11-D4 was 5.81 nmol·L-1 based on the hypothesis that the expression level of H11-D4 in the eukaryotic expression system was equal to that of Fe-H11-D4, and the neutralizing activity of eukaryotic expression was 29-fold higher than that of prokaryotic. Since the prokaryotic expression system does not have post-translational modification functions such as glycosylation and phosphorylation, the bioactivity of denatured proteins may be reduced after renaturation because they cannot revert to the correct folding mode of natural products. However, the exogenous protein expressed in the eukaryotic expression system does not need a denaturation and renaturation process and has the function of post-translational processing and modification. The function of ferritin nanocages to display polyproteins can be used to the maximum extent by using the baculovirus expression system.

The recombinant proteins expressed in the silkworm baculovirus expression system with 10-fold higher yields than those of the Ac-SF cell system, and the production cost can be reduced by more than a hundredfold.[31,32] This system has the advantages of low production cost, high expression level, and does not involve live harmful viruses in the preparation process. Compared with the conventional antibody production method, it is safer and simpler to operate and more suitable for rapid large-scale production. The fusion expression of nanobody H11-D4 with human ferritin broadens the

application range of ferritin self-assembly technology in vaccine and drug production. Fenobody also provides a reference for the subsequent production of neutralizing antibodies and the development of vaccines. This study laid a foundation for the establishment of a low-cost, high-neutralizing drug for the diagnosis and treatment of other important epidemic viruses.

Conclusion

The nanobody was displayed on the surface of ferritin, which effectively improved the targeting affinity of the nanobody to RBD and the neutralizing activity of the nanobody against pseudoviruses. The fenobodies can self-assemble well in silkworms, and the neutralizing activity of fenobody expressed in silkworms was significantly higher than that expressed in prokaryotic.

Acknowledgments

This work was supported by the National Key Research and Development Program of China (No. 2022YFD1300700), the National Natural Sciences Foundation of China (No. 32372952, 32072796, 32002236), the Agricultural Science and Technology Innovation Program of the Chinese Academy of Agricultural Sciences (CAAS-ZDRW202305), and the Regional Demonstration Project of Huzhou Academy of Agricultural Sciences Alliance (No. 2022SJLM10).

Disclosure

National Invention Patents, SARS-CoV-2 neutralizing nanobody, self-assembled ferritin fusion nanobody and preparation method and application, Li Yinü, Zhang Zhifang, Liu Xingjian, Gao Xintao, Yi Yongzhu, Wang Haining, 20220614, CN1, 20220902, ZL 2022 1 0663315.9. The authors report no other conflicts of interest in this work.

References

1. Kirtipal N, Bharadwaj S, Kang SG. From SARS to SARS-CoV-2, insights on structure, pathogenicity, and immunity aspects of pandemic human coronaviruses. *Infect Genet Evol*. 2020;85. doi:10.1016/j.meegid.2020.104502
2. Wrapp D, Wang NS, Corbett KS, et al. Cryo-EM structure of the 2019-nCoV spike in the prefusion conformation. *Science*. 2020;367(6483):1260–+. doi:10.1126/science.abb2507
3. Hassanzadeh-Ghassabeh G, Devoogdt N, De Pauw P, Vincke C, Muyldermans S. Nanobodies and their potential applications. *Nanomedicine*. 2013;8(6):1013–1026. doi:10.2217/Nnm.13.86
4. Hamers-Casterman C, Atarhouch T, Muyldermans S, et al. Naturally occurring antibodies devoid of light chains. *Nature*. 1993;363(6428):446–448. doi:10.1038/363446a0
5. Bannas P, Hambach J, Koch-Nolte F. Nanobodies and nanobody-based human heavy chain antibodies as antitumor therapeutics. *Front Immunol*. 2017;8. doi:10.3389/fimmu.2017.01603
6. Van Bockstaele F, Holz JB, Revets H. The development of nanobodies for therapeutic applications. *Curr Opin Invest Dr*. 2009;10(11):1212–1224.
7. Steeland S, Vandenbroucke RE, Libert C. Nanobodies as therapeutics: big opportunities for small antibodies. *Drug Discovery Today*. 2016;21(7):1076–1113. doi:10.1016/j.drudis.2016.04.003
8. Hanke L, Perez LV, Sheward DJ, et al. An alpaca nanobody neutralizes SARS-CoV-2 by blocking receptor interaction. *Nat Commun*. 2020;11(1). doi:10.1038/s41467-020-18174-5
9. Huo J, Le Bas A, Ruza RR, et al. Neutralizing nanobodies bind SARS-CoV-2 spike RBD and block interaction with ACE2. *Nat Struct Mol Biol*. 2020;27(9):846–854. doi:10.1038/s41594-020-0469-6
10. Fan K, Jiang B, Guan Z, et al. Fenobody: a ferritin-displayed nanobody with high apparent affinity and half-life extension. *Anal Chem*. 2018;90(9):5671–5677. doi:10.1021/acs.analchem.7b05217
11. Powell AE, Zhang KM, Sanyal M, et al. A single immunization with spike-functionalized ferritin vaccines elicits neutralizing antibody responses against SARS-CoV-2 in mice. *Acs Central Sci*. 2021;7(1):183–199. doi:10.1021/acscentsci.0c01405
12. Cho KJ, Shin HJ, Lee JH, et al. The crystal structure of ferritin from reveals unusual conformational changes for iron uptake. *J Mol Biol*. 2009;390(1):83–98. doi:10.1016/j.jmb.2009.04.078
13. Han JA, Kang YJ, Shin C, et al. Ferritin protein cage nanoparticles as versatile antigen delivery nanoplatforms for dendritic cell (DC)-based vaccine development. *Nanomed Nanotechnol*. 2014;10(3):561–569. doi:10.1016/j.nano.2013.11.003
14. Torti FM, Torti SV. Regulation of ferritin genes and protein. *Blood*. 2002;99(10):3505–3516. doi:10.1182/blood.V99.10.3505
15. Harrison PM, Arosio P. Ferritins: molecular properties, iron storage function and cellular regulation. *BBA-Bioenergetics*. 1996;1275(3):161–203. doi:10.1016/0005-2728(96)00022-9
16. Felberbaum RS. The baculovirus expression vector system: a commercial manufacturing platform for viral vaccines and gene therapy vectors. *Biotechnol J*. 2015;10(5):702–785. doi:10.1002/biot.201400438
17. van Oosten L, Altenburg JJ, Fougeroux C, et al. Two-component nanoparticle vaccine displaying glycosylated spike S1 domain induces neutralizing antibody response against SARS-CoV-2 variants. *Mbio*. 2021;12(5). doi:10.1128/mBio.01813-21
18. Geisler C, Mabashi-Asazuma H, Jarvis DL. An overview and history of glyco-engineering in insect expression systems. *Methods Mol Biol*. 2015;1321:131–152. doi:10.1007/978-1-4939-2760-9_10

19. Jumper J, Evans R, Pritzel A, et al. Highly accurate protein structure prediction with AlphaFold. *Nature*. 2021;596(7873):583–+. doi:10.1038/s41586-021-03819-2
20. Liu XJ, Yang X, Mehboob A, et al. A construction strategy for a baculovirus-silkworm multigene expression system and its application for coexpression of type I and type II interferons. *Microbiologyopen*. 2020;9(3):e979. doi:10.1002/mbo3.979
21. Liu XJ, Wei YL, Li YN, et al. A highly efficient and simple construction strategy for producing recombinant baculovirus nucleopolyhedrovirus. *PLoS One*. 2016;11(3). doi:10.1371/journal.pone.0152140
22. Hu J, Gao QZ, He CL, Huang AL, Tang N, Wang K. Development of cell-based pseudovirus entry assay to identify potential viral entry inhibitors and neutralizing antibodies against SARS-CoV-2. *Genes Dis*. 2020;7(4):551–557. doi:10.1016/j.gendis.2020.07.006
23. Wu CH, Xu Q, Wang HY, et al. Neutralization of SARS-CoV-2 pseudovirus using ACE2-engineered extracellular vesicles. *Acta Pharmaceutica Sinica B*. 2022;12(3):1523–1533. doi:10.1016/j.apsb.2021.09.004
24. Van Heeke G, Allosery K, De Brabandere V, De Smedt T, Detalle L, de Fougerolles A. Nanobodies® as inhaled biotherapeutics for lung diseases. *Pharmacol Therapeut*. 2017;169:47–56. doi:10.1016/j.pharmthera.2016.06.012
25. Luiz MB, Pereira SS, Prado NDR, et al. Camelid Single-Domain Antibodies (VHHs) against crotoxin: a basis for developing modular building blocks for the enhancement of treatment or diagnosis of crotalic envenoming. *Toxins*. 2018;10(4). doi:10.3390/toxins10040142
26. Roovers RC, Vosjan MJWD, Laeremans T, et al. A biparatopic anti-EGFR nanobody efficiently inhibits solid tumour growth. *Int J Cancer*. 2011;129(8):2013–2024. doi:10.1002/ijc.26145
27. Deckers N, Saerens D, Kanobana K, et al. Nanobodies, a promising tool for species-specific diagnosis of cysticercosis. *Int J Parasitol*. 2009;39(5):625–633. doi:10.1016/j.ijpara.2008.10.012
28. Wang W, Zhou X, Bian Y, et al. Dual-targeting nanoparticle vaccine elicits a therapeutic antibody response against chronic hepatitis B. *Nature Nanotechnol*. 2020;15(5):406–416. doi:10.1038/s41565-020-0648-y
29. López-Sagaseta J, Malito E, Rappuoli R, Bottomley MJ. Self-assembling protein nanoparticles in the design of vaccines. *Comput Struct Biotec*. 2016;14:58–68. doi:10.1016/j.csbj.2015.11.001
30. Li D, Song HZ, Li JL, et al. Expression and evaluation of a novel PPRV nanoparticle antigen based on ferritin self-assembling technology. *Pharmaceutics*. 2022;14(9). doi:10.3390/pharmaceutics14091902
31. Usami A, Suzuki T, Nagaya H, Kaki H, Ishiyama S. Silkworm as a Host of Baculovirus Expression. *Curr Pharm Biotechno*. 2010;11(3):246–250. doi:10.2174/138920110791112013
32. Usami A, Ishiyama S, Enomoto C, et al. Comparison of recombinant protein expression in a baculovirus system in insect cells (Sf9) and silkworm. *J Biochemi*. 2011;149(2):219–227. doi:10.1093/jb/mvq138